The Journal of Experimental Biology 207, 3619-3628
Published by The Company of Biologists 2004
doi:10.1242/jeb.01187

Transmission of linearly polarized light in seawater: implications for polarization signaling

Nadav Shashar[1,2,*], Shai Sabbah[1,2] and Thomas W. Cronin[3]

[1]*The Inter University Institute for Marine Sciences in Eilat, PO Box 469, Eilat 88103, Israel*, [2]*ESE Department, Life Sciences Institute, The Hebrew University, Jerusalem 91904, Israel* and [3]*Department of Biological Sciences, University of Maryland Baltimore County, 1000 Hilltop Road, Baltimore, MD 21250, USA*

*Author for correspondence (e-mail: nadavs@huji.ac.il)

Accepted 12 July 2004

Summary

Partially linearly polarized light is abundant in the oceans. The natural light field is partially polarized throughout the photic range, and some objects and animals produce a polarization pattern of their own. Many polarization-sensitive marine animals take advantage of the polarization information, using it for tasks ranging from navigation and finding food to communication. In such tasks, the distance to which the polarization information propagates is of great importance. Using newly designed polarization sensors, we measured the changes in linear polarization underwater as a function of distance from a standard target. In the relatively clear waters surrounding coral reefs, partial (%) polarization decreased exponentially as a function of distance from the target, resulting in a 50% reduction of partial polarization at a distance of 1.25–3 m, depending on water quality. Based on these measurements, we predict that polarization sensitivity will be most useful for short-range (in the order of meters) visual tasks in water and less so for detecting objects, signals, or structures from far away. Navigation and body orientation based on the celestial polarization pattern are predicted to be limited to shallow waters as well, while navigation based on the solar position is possible through a deeper range.

Key words: partial linear polarization, polarization sensitivity, navigation, vision, communication.

Introduction

Of the three fundamental properties of light [intensity (or the rate of photon arrival), wavelength or spectrum (often interpreted as hue or color) and polarization], polarization is the least known to the general public. This is because humans are mostly insensitive to the polarization characteristics of light (although we use them in sunglasses, computer screens, digital displays, etc.). However, many animals, terrestrial and marine, are sensitive to the polarization of light and make use of this polarization sensitivity for a variety of tasks. In a simplified way, polarization can be described as the distribution of the planes of vibration (the orientation of polarization) of the electrical (or magnetic) fields of the electromagnetic waves within a light beam. Partially linearly polarized light can be conceived as a mixture of fully linearly polarized light, with the plane of vibration of its electric vector (*e*-vector) at a given orientation (angle), called the *e*-vector orientation, combined with fully depolarized light, having random *e*-vector orientations. The fraction of the fully polarized component is the partial polarization, often represented as a percentage (% polarization). Thus, linear polarization has three descriptors: intensity, partial polarization and orientation of polarization.

The distribution of polarized light underwater is predominantly affected by the position of the sun (or the moon) in the sky, the optical properties of the water, the depth of viewing and reflections from surfaces, such as the sea floor or the surface of the water (Waterman, 1955, 1988; Waterman and Westell, 1956; Tyler, 1963; Timofeeva, 1969, 1970; Novales-Flamarique and Hawryshyn, 1997; Cronin and Shashar, 2001). Measurements performed at depths of 5–6 m by Waterman (1954) revealed that underwater there are two distinct polarization patterns, one inside Snell's window and one outside it. Generally, the polarization pattern inside Snell's window down to depths of a few meters is assumed to be determined by the same factors as those influencing the sky polarization. Therefore, sun position, amount of overcast, amount of atmospheric dust, the distance of the point observed from the zenith, multiple scattering, and depolarization due to anisotropy of air molecules will all influence the polarization pattern within Snell's window (Waterman, 1981, 1988).

Horvath and Varju (1995) modeled the underwater polarization pattern within Snell's window as it correlates to the celestial polarization pattern, taking into account

refraction and repolarization of skylight at the air–water interface. However, due to the focusing and defocusing of sunlight by surface waves (Schenck, 1957; Snyder and Dera, 1970; Stramska and Dickey, 1998; Maximov, 2000) and changes in polarization as the light propagates in water, certain distortions may well occur. Indeed, Cronin and Shashar (2001), measuring polarization at a depth of 15 m on a coral reef, found only small differences between the polarization patterns within Snell's window and outside it. Underwater, factors such as turbidity, bottom reflection (Ivanoff and Waterman, 1958) and proximity to the shore line (Schwind, 1999) may diminish the percent polarization. In shallow waters, the percent polarization first decreases with depth (Ivanoff and Waterman, 1958) and then reaches a depth-independent value (Timofeeva, 1974). Assuming primarily Raleigh scattering, Waterman and Westell (1956) proposed a model for the effect of the sun's position on the *e*-vector orientation outside Snell's window (see also illustration in Hawryshyn, 1992). However, with increasing depth, the pattern of *e*-vector orientation simplifies rapidly, tending to become horizontal everywhere (Waterman, 1955; Tyler, 1963; Timofeeva, 1969). It also diverges from the predictions of Waterman and Westell's model (Waterman and Westell, 1956) suggesting an effect on polarization of other, non-Raleigh, modes of scattering and of post-scattering processes. Within this complex partially polarized light field, animals use polarization sensitivity for a wide range of tasks.

Polarization imaging, combined with intensity imaging, can increase the detection range of objects in a scattering medium, including those that reflect polarized light (Briggs and Hatcett, 1965; Lythgoe and Hemming, 1967; Lythgoe, 1971; Rowe et al., 1995; Tyo et al., 1996; Chang et al., 2003), transparent objects (Shashar et al., 1995) and non-polarizing objects (Cariou et al., 2003; Chang et al., 2003; Schechner and Karpel, 2004). Fish and squid exploit this phenomenon, using polarization vision to improve the range of detection of transparent prey (Novales-Flamarique and Browman, 2001; Shashar et al., 1998). Animals such as shrimps, the freshwater branchiopod *Daphnia* and possibly fish also use the underwater polarized light field for navigation or for escaping towards or away from shore (Goddard and Forward, 1991; Ritz, 1991; Hawryshyn, 1992; Schwind, 1999).

Some animals produce polarization patterns of reflected light that do not contain intensity patterns (in other words, they cannot be seen using imaging devices responding to intensity alone), which are apparently used for communication. Examples of such animals include stomatopod crustaceans (Marshall et al., 1999) and cephalopods (Shashar et al., 1996). Polarization signaling has been suggested to serve as a concealed means of communication used by polarization-sensitive animals that are preyed upon by polarization-insensitive predators (Shashar et al., 1996). Cronin et al. (2003a,b) postulated that polarization signals would be especially useful for animals needing to transfer information at different depths, because spectral signals will change according to the varying penetration of different wavelengths through water, while polarization will maintain high signal constancy. We wished to learn how polarization signals vary when seen from different distances in water or, more generally, how natural waters affect the propagation of patterns of polarized light.

Materials and methods

To examine how polarization changes as a function of distance in water, a polarization target was created. This ~1×1 m target consisted of two linear polarizing filters (Polaroid HN38S; sealed with heat and glue at the edges to remain stable underwater even under pressure) set at orthogonal orientations (vertical and horizontal, each equipped with a depolarizing filter at its back), a spectrally flat, highly reflective depolarizer (made of several layers of wax paper, which appeared white to the eye) and a sheet of plastic painted flat black. The target was set 0.5–1 m above the sea floor at different locations in the waters surrounding Lizard Island (LI; partially turbid waters; depth 5–18 m, visibility ~8 m) and in Dynamite Passage on the Great Barrier Reef (GBR; clear oceanic water; depth 6–8 m, visibility up to 40 m), Australia, representing waters of two very different levels of turbidity. Measurements were taken during September 2003 (southern hemisphere winter) between 10:30 h and 15:00 h local time, with the sun towards the north (sun bearings 51–295° through the north; sun position based on US Naval Observatory calculations; http://aa.usno.navy.mil/data/docs/AltAz.html) at altitudes of 44–67° (zenith is 90°). Skies were partly cloudy to different extents, but the sun and the surrounding region of sky were always exposed.

The target was videotaped over a range of distances (0.5–10 m near LI and 0.5–15 m at GBR) with a custom-built underwater imaging polarimeter. This imaging polarimeter, placed 80–100 cm above the sandy bottom (and thus centered on the target) was based on a Sony VX1000E digital video camera that used a Polaroid HN38S filter set in front of it, rotating automatically to 0°, 45° and 90° from horizontal (where 0° represents the filter being set horizontally). Exposure of the camera was set manually, thus maintaining constant settings throughout each measurement series, and measurements were performed near the middle of the camera's exposure range (Chiao et al., 2000). The camera and filter were placed inside an underwater housing equipped with a flat viewing port. Color video images from the three filter settings (i.e. 0°, 45° and 90°) were replayed and captured by computer, reduced into 8-bit gray-scale images and analyzed according to the equations of Wolff and Andreou (1995) to provide the percent (partial) polarization, orientation of polarization and intensity, throughout the image, on a single pixel basis (Fig. 1). The details of these calculations are provided elsewhere (Wolff and Andreou, 1995) but, in short, if I_0, I_{45} and I_{90} represent the intensity

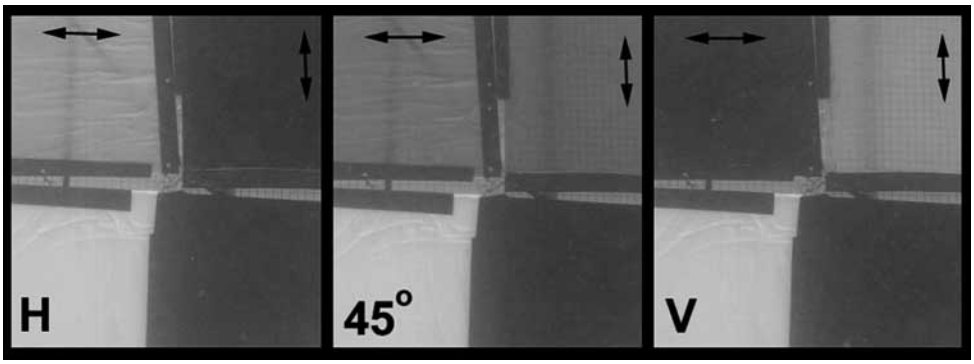

Fig. 1. The experimental polarization target as viewed underwater from a distance of 2 m through a linearly polarizing filter placed at horizontal (H; 0°), 45° and vertical (V; 90°) orientations. The target consisted of two upper panels made of horizontal and vertical polarizing filters (orientation of the transmitted *e*-vector indicated by arrows) and two lower panels made of a white depolarized standard and a flat-black standard.

values recorded when the polarizing filter was at 0°, 45° and 90°, respectively, then:

$$\text{Orientation of polarization} = 0.5\times\arctan[(I_0 + I_{90} - 2I_{45})/(I_{90} - I_0)]\pm 90° \quad (1)$$

and

$$\text{Partial polarization} = [(I_0 - I_{90})^2 + (2I_{45} - I_0 - I_{90})^2]^{0.5}/(I_0 + I_{90}) \; . \quad (2)$$

For each measurement, an area of no less than 1500 pixels was averaged to produce the appropriate reading. Six measurement series (each including measurements from the different sections of the target shown in Fig. 1) were obtained, three near LI and three in the clear waters of the GBR.

To measure the rate of decay of polarization at different wavelengths, we used a custom-built rapid spectral polarimeter (Fig. 2). This polarimeter uses three 600 μm-diameter, 10 m-long, UV–Vis transmitting fiber optics attached to a three-channel ADC1000-USB spectrometer (Ocean Optics, Duendin, FL, USA). The polarimeter allows for reading the spectra of the light arriving from the three fibers nearly simultaneously. The spectrometer was set for an integration time of 150 ms, and 30 spectra were averaged in each measurement. Dark noise correction was performed prior to any calculation. A restrictor providing an acceptance angle of 5° (in water) was attached to each fiber, in series with a linearly polarizing filter (Polaroid HNP'B) set at one of three orientations: 0°, 45° or 90°. The heads of the three fibers, including restrictors and filters, were set in an underwater housing such that they were spatially aligned in parallel. Custom software controlled data acquisition and polarization analysis over the wavelength range of 400–700 nm.

This sensor was placed underwater in front of the center of a 60×50 cm linear sheet polarizer (Polaroid HN38S; water sealed and equipped with a depolarizing filter at its back) producing vertical polarization. Since the fiber optic heads were 7 cm apart, with a 5° acceptance angle per fiber, all three fibers examined the target up to a distance of 5.25 m. Measurements were performed at 0.5 m intervals from 0.5 m to 4 m away from the target. Based on these measurements (eight measurements with three repetitions at each location), the rates of polarization decrease were calculated throughout the 400–700 nm spectral range. Due to depth limitations (resulting from the length of the fiber optics), measurements were performed only in shallow waters (4–6 m deep), on two different days, near Horseshoe Reef, LI. On one of these occasions, a second set of measurements was obtained under nearly identical conditions using the video polarimeter and the 4-part target shown in Fig. 1.

Data were processed and analyzed using Microsoft Excel 2000® and Statistica 6.0® software.

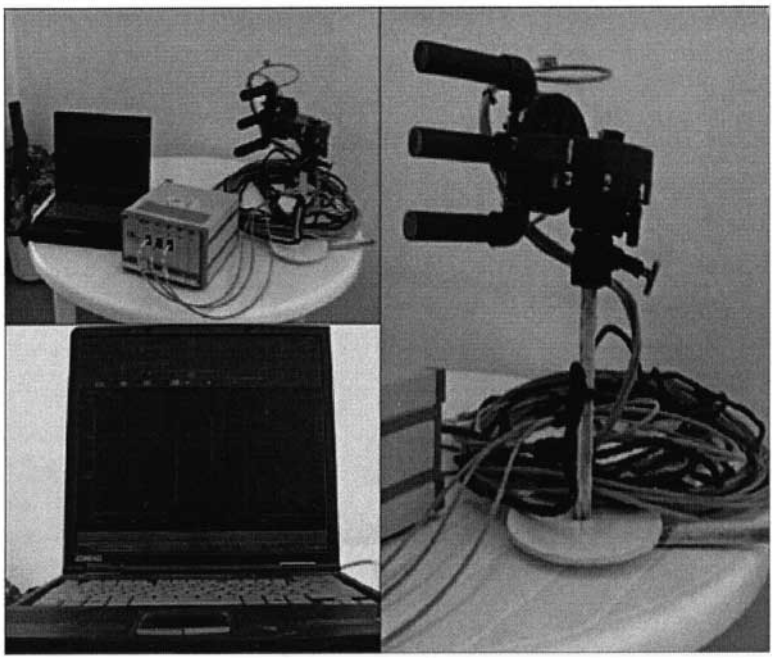

Fig. 2. The rapid spectral polarimeter used in this research. The sensor is based on three aligned fiber optics viewing an acceptance angle of 5° in water, each equipped with a linear polarizing filter set at a different orientation, encased in an underwater housing (right), and connected to a multi-channel Ocean Optics spectrometer and a portable computer for online control of the spectrometer and data acquisition (left).

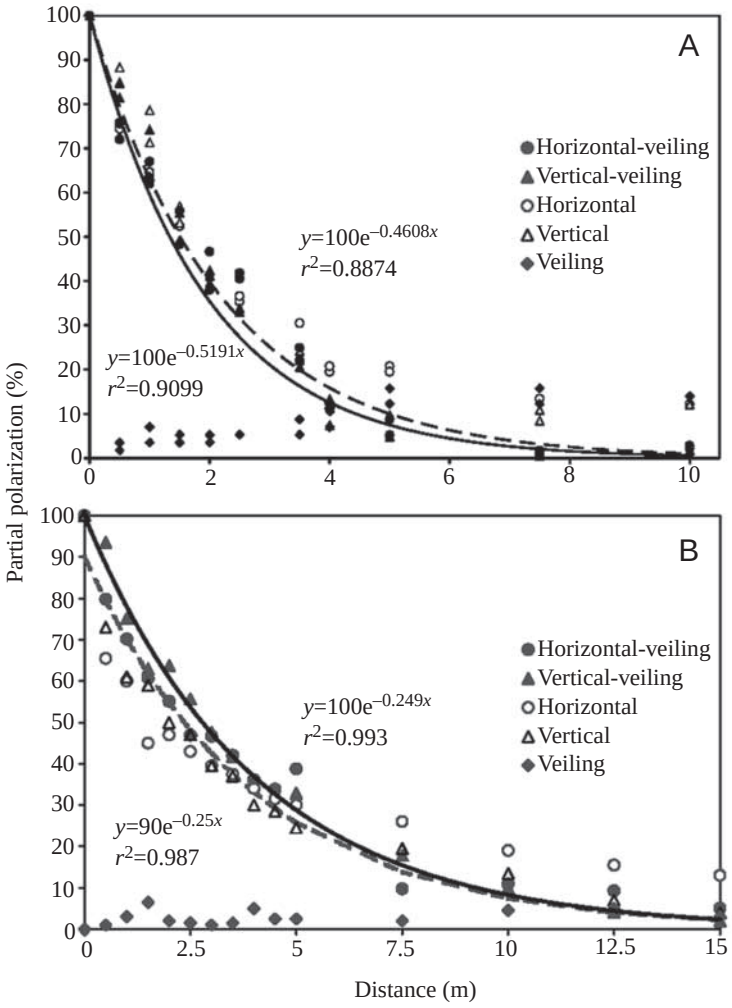

Fig. 3. Results of individual partial polarization measurement sets (duplicate measurements) of a standard target (Fig. 1) taken at different distances at (A) Horseshoe Reef, Lizard Island (~5 m deep) on 8 September 2003 and (B) Cod Hole, Great Barrier Reef (~7 m deep; 1 m above a sandy bottom) on 12 September 2003. Horizontal polarization decay (○) appears to be lower than that of vertical polarization (△). However, after vectorially subtracting the partial polarization arising from downwelling light [as measured from the depolarizing section of the target (◆)], the horizontal polarization decay (●; horizontal-veiling) becomes similar to that of the vertical polarization (▲; vertical-veiling), and they both fit an exponential decay (broken and continuous lines, respectively). Background polarization was ~9% in both cases.

Results

Using the video polarimeter, we obtained four sets of polarization measurements (each including percent and orientation of polarization) at each target range and point in time, corresponding to the four sections of the target. Light arriving from the direction of polarizing sections demonstrated the changes occurring to a polarization signal as it travels in water, while light coming from the direction of the depolarized sections (black-and-white panels) provided information as to the induced polarization caused by veiling light (downwelling light that is scattered between the target and the sensor and that reaches the sensor). Naturally, the latter process also affects the measurements taken from the polarizing sections, but it can be removed using vectorial subtraction. Unfortunately, due to the very low readings measured from the black section, we could not reliably calculate the polarization characteristics of light coming from it and hence used only values obtained from the white section.

The partial (percent) polarization of light arriving from the polarization filters of the target decreased with distance (Fig. 3), while that coming from the direction of the depolarized section increased (Spearman's correlation test, $P>0.8$ in all cases, 0.97 for Fig. 3A, 0.81 for Fig. 3B). Eventually, all measurements reached, or were close to (statistically indistinguishable from), the level of the background polarization. The decrease in partial polarization could, in all cases, be described using an exponential function ($r^2>0.88$ in all cases; $N=12$; composed of two measurement sets, one taken from the vertical and the other from the horizontal polarizing panels of the target, at each of six measurement series performed; each series taken at a different time, place or line of site) following the general equation $P_z=P_0\cdot e^{-Z\cdot c_p}$, where P_0 represents the original partial polarization (in our case postulated to be 100%, except for 90% in one case; i.e. that of the polarizers in the target), P_z represents the partial polarization at a distance of z (here, in meters) from the target, and c_p represents the polarization extinction coefficient per meter.

The partial polarizations of the horizontally and vertically polarizing targets (after vectorially subtracting the polarization added by the scattering of downwelling light as measured from the depolarizing target) were very similar at each target distance, and so were their polarization extinction coefficients (Fig. 3). c_p values were calculated for each of the 12 measurement sets taken from the vertical and horizontal polarizing panels (after correction for polarization in the veiling illumination) and used for further analysis. c_p values of horizontal or vertical polarization were not significantly different (for partly turbid waters: c_p horizontal = $0.54\pm0.06\ m^{-1}$; c_p vertical = $0.54\pm0.03\ m^{-1}$; mean ± S.D.; Student's t-test, $P>0.5$) and hence were grouped together. c_p values for sandy bottom areas with medium visibility of approximately 8 m, such as those surrounding LI, were $0.54\pm0.04\ m^{-1}$ ($N=6$), while in the very clear waters of the GBR, with visibility estimated at 40 m, c_p values were lower, averaging $0.24\pm0.05\ m^{-1}$ ($N=6$).

Regarding the polarization orientation, near the targets the observed *e*-vector angles were those of the filters themselves (i.e. horizontal or vertical), while the orientation of the limited polarization that arose from veiling illumination (as measured in front of the depolarizing standard) was predominantly near the horizontal (e.g. near 160°; Fig. 4). As the partial (percent)

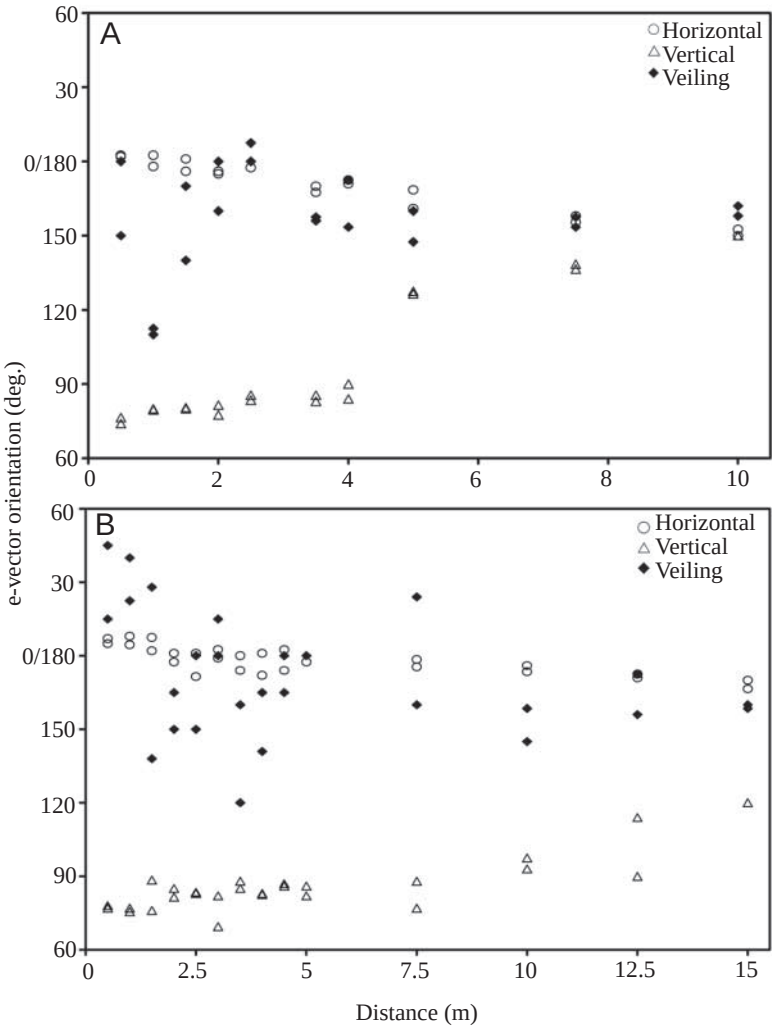

Fig. 4. Results of individual orientation of polarization measurement sets (duplicate measurements) of a standard target (Fig. 1) taken as in Fig. 3. 0/180° represents horizontal orientation, and 90° represents vertical orientation. For convenience, the scale starts and ends at 60°. Measurements reveal that the vertical panel was not perfectly oriented to the desired (90°) position in relation to the sensor. Veiling light measurements (◆) at short distances from the target with low partial polarization (see Fig. 3) should not be considered as reliable. Further away from the target, the light coming from the vertically polarizing panel (△) and the horizontally polarizing panel (○) converge onto the veiling light's *e*-vector orientation. Background polarization's *e*-vector orientation was 161° in A and 164° in B.

polarization of the light coming from the target became lower with distance, and the effect of the veiling illumination became higher, the orientation of polarization of all parts of the target converged onto that of the veiling light (Fig. 4) and therefore also onto that of the background light.

c_p varied with wavelength (Fig. 5), with highest values in the shorter (blue) range and the lowest values in the wavelength range between ~510 and ~580 nm.

Modeling polarization pattern propagation

The results we obtained in this study encouraged us to formulate a general model for the formation of polarized light fields in water. Such a model can be useful for explaining (and predicting) the patterns of polarization seen in natural waters. Here, we present the model for horizontal lines of sight; with some effort, it can be, in principle, generalized to any direction of view outside of Snell's window, with appropriate corrections for the changing intensities of light at different depths along the line of sight and the changing scattering angles (between the generally downwelling light and the line of sight).

Consider the scattering of light perpendicular to a horizontal line of sight. If the water is homogeneous, at sufficient depth one can assume illumination to be equivalent at each position along a given line of sight. This assumption is generally true at depths below the influence of localized effects caused by the focusing or defocusing of downwelling light by waves (Schenck, 1957; McFarland and Loew, 1983; Stramska and Dickey, 1998; Maximov, 2000) or by reflections from objects or the substrate. In such constant conditions of illumination, the amount of light scattered in each infinitesimally thin distance plane is identical, and some constant fraction (P_s) of this light is polarized. Let us designate the intensity of the scattered light at each point as I_o. Then, the amount of light that is polarized is $I_o \times P_s$. As the light travels from the point of scattering to the viewer, a distance designated by z, the beam of light is attenuated by water by the standard equation:

$$I_z = I_o \cdot e^{-c \cdot z} \ . \qquad (3)$$

Here, c represents the beam attenuation coefficient (Jerlov, 1976). Simultaneously, the polarization of the light is reduced along the path by scattering, according to the polarization attenuation coefficient c_p, and the remaining polarized light continues to be attenuated according to the beam attenuation coefficient c. Thus:

$$I_{pz} = I_o \cdot P_s \cdot e^{-c \cdot z} \cdot e^{-c_p \cdot z} = I_o \cdot P_s \cdot e^{-(c + c_p) \cdot z} \ , \qquad (4)$$

where I_{pz} represents the intensity of the polarized light reaching the viewer from a particular scattering plane at distance z. Therefore, the overall partial polarization, P_z, viewed along the line of sight from an observer to a point at distance z is simply the integral of the polarized light arriving from all intervening scattering planes divided by the integral of all light; since I_o appears in both terms it cancels out (the partial polarization is therefore independent of intensity, as expected):

$$P_z = P_s \cdot ({}_0\textstyle\int^z (e^{-(c + c_p) \cdot z}\, dz) / {}_0\textstyle\int^z e^{-c \cdot z}\, dz) \ , \qquad (5)$$

where P_z is the partial polarization observed at a range of z in a certain horizontal line of view or direction, and P_s is (as above) the partial polarization of the light that is scattered at

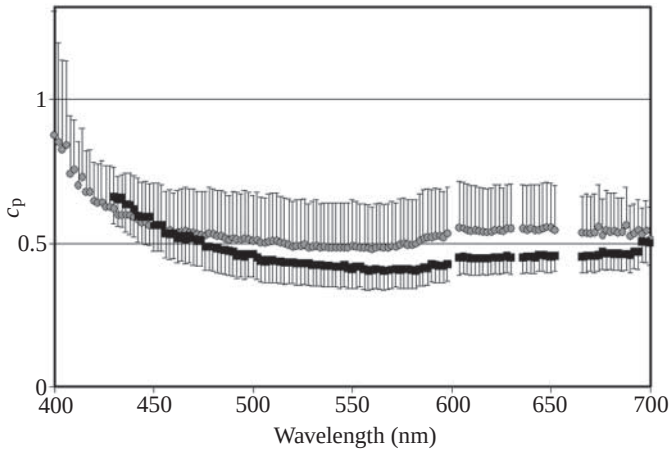

Fig. 5. Partial polarization extinction coefficients (c_p) per meter at different wavelengths (mean ± S.D.) calculated from measurements taken at distances of 0.5–4 m, at 0.5 m intervals, of a vertically polarizing filter set 80 cm above a sandy bottom, near Horseshoe Reef, Lizard Island, on two different days [8 September 2003 (squares) and 10 September 2003 (circles)]. The mean c_p across the 400–700 nm range was 0.47±0.06 for 8 September and 0.55±0.07 for 10 September. The measurements on 8 September were taken at the same time and location as Figs 3A, 4A. The 'gray-scale' c_p (i.e. that measured using the video system, combining the R, G and B images) corresponding to this measurement was 0.49 (Fig. 3A).

each point along the line of view. c_p is the polarization extinction coefficient, as described in the results, and c is the beam (intensity) attenuation coefficient in the water (Jerlov, 1976). P_s, or the partial polarization induced at the point of scattering of downwelling light, varies with the angle of scattering (where it is lowest in forward scattering and highest at side scattering) and with the scattering properties of the medium (Timofeeva, 1970). Here, we examine only the horizontal line of view and hence are interested only in the side scattering (scattering to a direction perpendicular to the direction of the incoming light). Ivanoff and Waterman (1958) report that the maximal P_s varies from 45 to 77% in seawater but it can reach a level of 80% in pure water and up to 88% in certain turbid solutions. Solving the integrals:

$$P_z = [P_s/(1 + c_p/c)][1 - e^{-(c + c_p)\cdot z}]/(1 - e^{-c\cdot z}) \ . \quad (6)$$

At infinity, we therefore obtain:

$$P_\infty = P_s/(1 + c_p/c) \ , \quad (7)$$

where P_∞ is the partial polarization of the background light in water assuming there is no obstacle in the line of sight. In practicality, a clear optical path in the order of the visibility range is sufficient for obtaining such values (see also Timofeeva, 1974).

This model allows us to predict the partial polarization in the water along horizontal lines of sight (P_∞), where there are no surface effects (e.g. Schenck, 1957) nor reflection from the bottom (i.e. in midwater), and to relate it to the inherent optical properties of the beam attenuation coefficient (c), the polarization induced by side scattering (P_s) and the polarization attenuation coefficient (c_p)

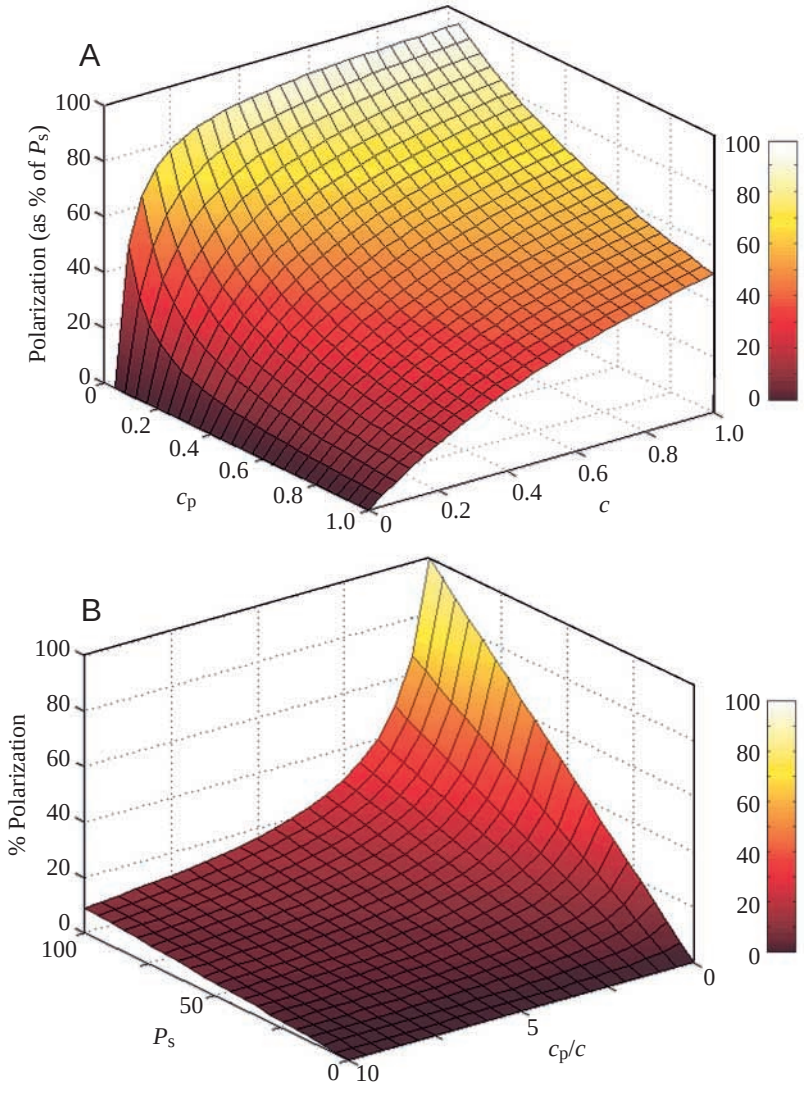

Fig. 6. Analysis of the P_∞ (% polarization) seen in the horizontal direction in clear midwater. (A) Partial polarization (as the percentage of P_s; the polarization induced by side scattering) as a function of c_p (the polarization attenuation coefficient, measured in this work) and c (the beam attenuation coefficient). (B) Predicted partial (%) polarization, based on equation 7 (see text). This analysis plots % polarization as a function of c_p/c and P_s. In nature, P_s ranges from very low values to ~85%, depending on water quality and the nature of the suspended scattering particles.

(Fig. 6A). The percent of partial polarization is favored by increases in c and by decreases in c_p and is therefore primarily dependent on the ratio c_p/c; see Fig. 6B. According to Jerlov (1976), beam attenuation in coastal waters, in the spectral range from 440 to 700 nm, varies from ~0.1 to ~1.0 m^{-1}. As noted above, P_s ranges from ~50% to ~80% (Ivanoff and Waterman, 1958). In the present study, we measured c_p as ~0.3 to 0.5 m^{-1} in fairly clear coastal waters. Since P_s, c_p and c are all influenced by water clarity and the type of material suspended in water, they are closely interrelated. However, one should note that while c and c_p are inherent optical properties of the water, P_s is influenced by the illumination conditions (such as the orientation of the sun) and should be considered as an apparent optical property of the water.

Discussion

Several processes affect a polarization light signal (the term 'signal' is intended as a distinct unit containing information and is not necessarily related to communication) as it propagates in water. The intensity of the light is reduced due to absorption and scattering. The partial polarization is reduced due to forward scattering (for discussion of forward and side scattering and their interaction with polarization, see Hechet, 1998). Veiling light, caused by in-path side scattering of downwelling light, is introduced between the target and the observer and makes it harder to detect the original signal (Lythgoe, 1979). At large distances, the veiling light is identical to the ambient background light in the water. This veiling light is partly polarized at orientations often close to, though not necessarily exactly, horizontal; so while the first two processes affect all orientations of polarization of the signal equally, veiling light has an inherent polarization orientation and hence may change the orientation of polarization of the light reaching an observer. All of these processes are wavelength dependent and vary with time of day, the clarity of the water, the types of materials dissolved or suspended in it, and the sizes and shapes of scatterers in the water.

Scattering creates two interacting effects on polarization propagation. On the one hand, forward scattering gradually depolarizes the original signal. On the other hand, side scattering introduces polarization due to the strong directionality (usually near overhead) of the downwelling light (Fig. 3). Although both processes tend to reduce the original signal, the interactions between them, together with the polarization of the background illumination, determine the polarization contrast level available to a polarization-sensitive animal.

The magnitude of the effects that these processes have on the original signal depends on the optical path length between the target and the observer. However, assuming a homogeneous medium, they are not dependent either on the direction or on the section of the path that is examined. Hence, the mathematical description of these effects is expected to be exponential in nature (Lythgoe, 1971). Our measurements of partial polarization decay indeed follow the exponential equation $P_z=P_0 \cdot e^{-z \cdot c_p}$. The propagation of partial polarization depends heavily on the scattering of the medium in which it travels. In the partly turbid waters near LI, which could be considered as representing moderately clear coastal waters, the decay was fairly rapid in nature, with nearly half of the partial polarization being lost with each 1.25 m traveled through water. This decay was lower in the clear oceanic waters of the GBR; yet even here, 50% polarization loss occurred at only 3 m or, to put it differently, only 10% of the original polarization was left after 4.1 and 10 m, respectively, in these two types of water. There was no difference in the extinction of partial polarization of the different orientations, with proper accounting for the effects caused by the addition of low levels of partly polarized veiling light. In our work, the downwelling light was nearly horizontally polarized, deviating no more than 20° from the horizontal plane, but different lines of sight would have different orientations of polarization depending primarily on the sun's position and visibility within Snell's window and on the water depth (Waterman and Westell, 1956; Waterman, 1988; Hawryshyn, 1992; Cronin and Shashar, 2001). It should be noted that since these measurements were made near the bottom, where sediment is continuously resuspended by currents and diver activity, they are probably somewhat greater in value than might be found higher up in the water column.

Based on these results, it is reasonable to predict that polarization patterns (including the celestial polarization pattern) will not propagate very far in water. Novales-Flamarique and Hawryshyn (1997) found that, even in shallow waters, the polarization of the light within Snell's window is lower than in air and that it further decreases with depth. Therefore, underwater navigation based on the celestial polarization pattern will be limited, at least near the coast, to shallow water. However, as the polarization orientation of the background illumination (produced in the water itself) is dependent on the position of the sun (Waterman and Westell, 1956; Waterman, 1988; Cronin and Shashar, 2001), animals may be able to use their polarization sensitivity for orientation in deeper waters. Other visual tasks, such as object detection and communication, are likely to be much less depth dependent, as the underwater light field is likely to be partially polarized throughout the photic zone (Waterman, 1955; Tyler, 1963).

In several cases, a biologically important polarization contrast arises from an object being less polarized than the background. Such cases may be reflections off fish (Shashar et al., 2000) or light passing through transparent objects such as planktonic organisms (Shashar et al., 1998; Novales-Flamarique and Browman, 2001). In these cases, the depolarization of the original signal due to forward scattering will not reduce the polarization contrast between the target and the background; instead, light from the direction of the object will become increasingly polarized by the veiling polarization. The differences between the rates of such increase in polarization *vs* polarization loss due to scattering will determine whether such a depolarized target could be detected at a larger or shorter range than a polarized one. Hence, a polarization pattern produced by transparent depolarizing

objects is expected to behave differently from that of polarizing objects. The factors governing the propagation of such a depolarized signal and especially the effects of the brightness of the depolarizing object need further examination.

The change in partial polarization of light coming from a small object will be identical to that of the polarization coming from a large target. Hence, even in waters of relatively high values of c_p, polarization vision could be used for detecting or examining small objects or patterns at distances of relevance for the viewing animals (for example, small fish detecting planktonic prey at distances of centimeters; Novales-Flamarique and Browman, 2001).

The mathematical model presented here enables us to better understand the factors governing the partial polarization of the background illumination in open waters within the optical zone of the sea, distant from bottom effects and from heterogeneity in illumination at the surface on the ocean. The model focuses on the processes affecting the polarization following the initial scattering event. Hence, it is independent of the mode of scattering in the water (Raleigh *vs* Mie). One outcome of the model and especially of equation 7, as well as of work by Timofeeva (1974), is that in an optically homogeneous water column with a well-defined light source in a constant position (such as the conditions occurring in the lower part of the photic zone, where the patch of brightest light is close to overhead throughout the entire day; see Jerlov, 1976), the partial polarization of the background will not vary with depth. Reports by Ivanoff and Waterman (1958) and by Tyler (1963) tend to support this outcome, although information about changes in the solar position between measurements is not provided. The model predicts that background polarization (P_∞) depends on the ratio between c_p and c (Fig. 6B). Timofeeva (1970) found that P_∞ is related to a parameter she designated as T (also referred to as ε; Timofeeva, 1974), defined as the ratio between the scattering attenuation coefficient and the total (asymptotic) light attenuation coefficient. Hence, T ranges from 0 to 1. Our c_p and Timofeeva's ε both depend on the scattering properties of the media, although the two are not equivalent: c_p is an empirical value and ε is a theoretical one. It is reasonable to expect that c_p is strongly affected by scattering, and thus c_p and T may well be closely related. Understanding underwater polarization and its theoretical basis still requires a thorough understanding of how light is scattered, polarized and attenuated in natural waters.

P_s, T, c_p and c are wavelength dependent. Not surprisingly, the decrease in partial polarization with distance was therefore found to vary with wavelength (Fig. 5), most likely due to wavelength-dependent scattering and absorption of light in the water. Hence, it is highly possible that in different water types, such as green or brown coastal waters (Jerlov types 3 or 9; Jerlov, 1976), different wavelengths will best transmit a polarization signal. Our results show that, in the types of waters we examined, polarization decay is lowest in the 510–580 nm range. Ivanoff and Waterman (1958) reported little partial polarization variation with wavelength in the ambient light field, in the order of 5% out of an approximately 10–30% average partial polarization, with the minimal partial polarization occurring at 450–500 nm. Cronin and Shashar (2001) reported similar findings and interpreted these as demonstrating that the ambient (background) polarization is nearly constant across the visual spectrum. In cephalopods and stomatopods, polarization vision is based on photoreceptors with maximal sensitivity around 500 nm. Hence, the polarization sensitivity of these animals (species of which inhabit the waters we examined) is well suited for detecting polarization patterns, either for signaling or for target detection, functioning within the spectral range in which polarization patterns propagate fairly well, while background and veiling polarization are relatively low.

Polarization vision, and especially polarization signaling, has the potential to provide polarization-sensitive organisms with information that is concealed from polarization-insensitive animals. The stability of polarization signals with depth offers a potential advantage for polarization sensitivity over color vision, but our results also indicate that these signals are most effective at short range (i.e. no more than a few meters). The conditions in which polarization signals are used, the information they contain and the visual adaptations required for making use of this information require further investigation.

Our model allows one to predict the partial polarization of background illumination in the horizontal plane. This information is important since it sets the stage for polarization contrast functions such as prey detection. It is somewhat counterintuitive to find that the percentage of background polarization is positively correlated with c (Fig. 6A), primarily because greater levels of beam attenuation diminish the effect of polarization decrease by scattering of polarized light arriving from greater distances.

The amount of light that is partially polarized by side scattering (P_s) depends on the amount and type of scattering occurring in the water. It is therefore affected by the concentration, size, shape and heterogeneity of the scatterers in the water. Changes in the downwelling light distribution due to wave action may also change P_s. Our model is limited to the horizontal line of sight and assumes a homogenous medium and constant illumination conditions. Further measurements and calculations are required to verify actual values of the critical parameters in nature (i.e. c_p, c and P_s), to extend this model to the whole visual sphere, and to incorporate into it temporal and spatial variation in the illumination field.

Summarizing, we found that polarization patterns propagate to relatively short distances in seawater. Therefore, the visual tasks that make use of such patterns or their details are range-limited as well. Polarization signals will not be seen by distant observers, be they conspecifics or predators. Similarly, navigation, detection of prey and object recognition will be limited to the distances or depths at which the polarization patterns can be seen. This range limitation may be less important to small animals or animals with low visual acuity, but in large predators we suggest that polarization sensitivity

will be more useful for ambush predators or for those that are slow moving. Fast-swimming animals, or those who hunt prey at great range, would gain little from using polarization vision to detect objects.

List of symbols

- c beam attenuation coefficient
- c_p polarization extinction coefficient
- e electric vector (*e*-vector)
- I_0 intensity value recorded when polarizing filter set at 0° (horizontal)
- I_{45} intensity value recorded when polarizing filter set at 45°
- I_{90} intensity value recorded when polarizing filter set at 90° (vertical)
- I_o intensity of scattered light at each point along the line of view (no propagation distance)
- I_{pz} intensity of polarized light reaching the viewer from a particular scattering plane at distance z
- I_z intensity of light travelling distance z
- P_∞ partial polarization of background light in water assuming there is no obstacle in the line of sight
- P_0 partial polarization at distance 0
- P_s polarization induced by side scattering
- P_z partial polarization at distance z
- T ratio between the scattering attenuation coefficient and the total (asymptotic) light attenuation coefficient (Timofeeva, 1970)
- z distance light travels from point of scattering to viewer

We thank Errol Zarfati for construction of the polarization filter-rotating device, Tsyr-Huei Chiou for enthusiastic support at sea and in the laboratory, Gary Bernard, Emmanuel Boss, and Misha Vorobyev for useful discussions, and the hospitality of the Lizard Island Research Station, Australia. Comments by two anonymous reviewers greatly improved this manuscript. This study was partially supported by the US Air Force Office of Scientific Research, NSF Grant # IBN-0235820, BSF Grant # 1999040 and ISF Grant #550/03.

References

Briggs, R. O. and Hatcett, G. L. (1965). Techniques for improving underwater visibility with video equipment. *Ocean Sci. Ocean Eng.* **1&2**, 1284-1308.

Cariou, J., Jeune, B. L., Lotrian, J. and Guern, Y. (1990). Polarization effects of seawater and underwater targets. *Appl. Opt.* **29**, 1689-1695.

Chang, P. C. Y., Flitton, J. C., Hopcraft, K. I., Jakeman, E., Jordan, D. L. and Walker, J. G. (2003). Improving visibility depth in passive underwater imaging by use of polarization. *Appl. Optics.* **42**, 2794-2803.

Chiao, C. C., Osorio, D., Vorobyev, M. and Cronin, T. W. (2000). Characterization of natural illuminants in forests and the use of digital video data to reconstruct illuminant spectra. *J. Opt. Soc. Am. A* **17**, 1713-1721.

Cronin, T. W. and Shashar, N. (2001). The linearly polarized light field in clear, tropical marine waters: spatial and temporal variation of light intensity, degree of polarization and *e*-vector angle. *J. Exp. Biol*. **204**, 2461-2467.

Cronin, T. W., Shashar, N., Caldwell, R. L., Marshall, J., Cheroske, A. G. and Chiou, T. H. (2003a). Polarization signals in the marine environment. In *Proceedings of SPIE 5158: Polarization Science and Remote Sensing* (ed. J. A. Shaw and J. S. Tyo), pp. 85-92. Bellingham, WA: SPIE Press.

Cronin, T. W., Shashar, N., Caldwell, R. L., Marshall, J., Cheroske, A. G. and Chiou, T. H. (2003b). Polarization vision and its role in biological signaling. *Int. Comp. Biol.* **43**, 549-558.

Goddard, S. M. and Forward, R. B. (1991). The role of the underwater polarized-light pattern, in sun compass navigation of the grass shrimp, *Palaemonetes vulgaris*. *J. Comp. Physiol. A* **169**, 479-491.

Hawryshyn, C. W. (1992). Polarization vision in fish. *Am. Sci.* **80**, 164-175.

Hechet, E. (1998). *Optics.* Reading, MA: Addison Wesley Longman, Inc.

Horvath, G. and Varju, D. (1995). Underwater refraction-polarization patterns of skylight perceived by aquatic animals through Snell's window of a flat-water surface. *Vision Res.* **35**, 1651-1666.

Ivanoff, A. and Waterman, T. H. (1958). Factors, mainly depth and wavelength, affecting the degree of underwater light polarization. *J. Mar. Res.* **16**, 283-307.

Jerlov, N. G. (1976). *Marine Optics*. Amsterdam: Elsevier.

Lythgoe, J. N. (1971). Vision. In *Underwater Science* (ed. J. D. Woods and J. N. Lythgoe), pp. 103-139. London: Oxford University Press.

Lythgoe, J. N. (1979). *The Ecology of Vision*. London: Oxford University Press.

Lythgoe, J. N. and Hemming, C. C. (1967). Polarized light and underwater vision. *Nature* **213**, 893-894.

Marshall, J., Cronin, T. W., Shashar, N. and Land, M. (1999). Behavioural evidence for polarisation vision in stomatopods reveals a potential channel for communication. *Curr. Biol.* **9**, 755-758.

Maximov, V. V. (2000). Environmental factors which may have led to the appearance of colour vision. *Phil. Trans. R. Soc. Lond. B* **355**, 1239-1242.

McFarland, W. N. and Loew, E. R. (1983). Wave produced changes in underwater light and their relations to vision. *Environ. Biol. Fish.* **8**, 173-184.

Novales-Flamarique, I. and Browman, H. I. (2001). Foraging and prey-search behaviour of small juvenile rainbow trout (*Onchorhychus* mykiss) under polarized light. *J. Exp. Biol*. **204**, 2415-2422.

Novales-Flamarique, I. and Hawryshyn, C. W. (1997). Is the use of underwater polarized light by fish restricted to crepuscular time periods? *Vision Res*. **37**, 975-989.

Ritz, D. A. (1991). Polarized-light responses in the shrimp *Palaemonetes vulgaris* (Say). *J. Exp. Mar. Biol. Ecol.* **154**, 245-250.

Rowe, M. P., Pugh, E. N., Jr, Tyo, J. S. and Engheta, N. (1995). Polarization difference imaging: a biologically inspired technique for observation through scattering media. *Opt. Lett.* **20**, 608-610.

Schechner, Y. and Karpel, N. (2004). Clear underwater vision. *Proc. IEEE Computer Vision and Pattern Recognition* **1**, 536-543.

Schenck, H. (1957). On the focusing of sunlight by ocean waves. *J. Opt. Soc. Am.* **47**, 653-657.

Schwind, R. (1999). *Daphnia pulex* swims towards the most strongly polarized light – a response that leads to 'shore flight'. *J. Exp. Biol*. **202**, 3631-3635.

Shashar, N., Adessi, L. and Cronin, T. W. (1995). Polarization vision as a mechanism for detection of transparent objects. In *Ultraviolet Radiation and Coral Reefs*. (ed. D. Gulko and P. L. Jokiel), pp. 207-212. Manoa, HI: HIMB and UNIHI-Sea Grant.

Shashar, N., Rutledge, P. S. and Cronin, T. W. (1996). Polarization vision in cuttlefish – a concealed communication channel? *J. Exp. Biol.* **199**, 2077-2084.

Shashar, N., Hanlon, R. T. and Petz, A. deM. (1998). Polarization vision helps detect transparent prey. *Nature* **393**, 222-223.

Shashar, N., Hagan R., Boal, J. G. and Hanlon, R. T. (2000). Cuttlefish use polarization sensitivity in predation on silvery fish. *Vision Res.* **40**, 71-75.

Snyder, R. L. and Dera, J. (1970). Wave-induced light-field fluctuations in the sea. *J. Opt. Soc. Am.* **6**, 1072-1079.

Stramska, M. and Dickey, T. D. (1998). Short-term variability of the underwater light field in the oligotrophic ocean in response to surface waves and clouds. *Deep Sea Res. I* **45**, 1393-1410.

Timofeeva, V. A. (1969). Plane of vibrations of polarized light in turbid media. *Izvestiya Atmos. Ocean. Physics* **5**, 603-607.

Timofeeva, V. A. (1970). The degree of polarization of light in turbid media. *Izvestiya Atmos. Ocean. Physics* **5**, 513-522.

Timofeeva, V. A. (1974). Optics of turbid waters. In *Optical Aspects of Oceanography* (ed. N. Jerlov and E. Steeman-Nielsen), pp. 177-218. New York: Academic Press.

Tyler, J. E. (1963). Estimation of percent polarization in deep oceanic water. *J. Mar. Res.* **21**, 102-109.

Tyo, J. S., Rowe, M. P., Pugh, E. N., Jr and Engheta, N. (1996). Target detection in optically scattering media by polarization-difference imaging. *Appl. Opt.* **35**, 1855-1870.

Waterman T. H. (1954). Polarization patterns in submarine illumination. *Science* **120**, 927-932.

Waterman, T. H. (1955). Polarization scattered sunlight in deep water. *Deep Sea Res.* **3(Suppl.)**, 426-434.

Waterman T. H. (1981). Polarization sensitivity. In *Comparative Physiology and Evolution of Vision in Invertebrates* (ed. H. Autrum), pp. 281-463. Berlin: Springer-Verlag.

Waterman, T. H. (1988). Polarization of marine light fields and animal orientation. *SPIE* **925**, 431-437.

Waterman, T. H. and Westell, W. E. (1956). Quantitative effects of the sun's position on submarine light polarization. *J. Mar. Res.* **15**, 149-169.

Wolff, L. B. and Andreou, A. G. (1995). Polarization camera sensors. *Image Vision Comput.* **13**, 497-510.